Scientific Research Publishing

International Journal of Geosciences, 2026, 17(9), 652-670
https://www.scirp.org/journal/ijg
ISSN Online: 2156-8367
ISSN Print: 2156-8359

# New U-Pb Zircon Evidence for Paleoarchean Crustal Inheritance in the Kenema-Man Domain, Western Côte d'Ivoire

**Wilfried Digbeu[1]*, Alain Nicaise Kouamelan[2], Koffi Alexis N'Dri[3], Ziandjêdé Hervé Siagné[3], Gnagnon Stéphane Raymond Koffi[2], Zié Ouattara[1]**

[1]Département de Géologie et Matériaux, UFR des Sciences Géologiques et Minières, Université de Man, Man, Côte d'Ivoire
[2]Laboratoire de Géologie, Ressources Minérales et Energétiques, Université Félix Houphouët-Boigny, Abidjan, Côte d'Ivoire
[3]Laboratoire des Sciences Géographiques, du Génie Civil et des Géosciences, Ecole Supérieure des Mines et Géologie, Institut National Polytechnique Félix Houphouët-Boigny, Yamoussoukro, Côte d'Ivoire
Email: *wilfrieddigbeu004@gmail.com

**How to cite this paper:** Digbeu, W., Kouamelan, A.N., N'Dri, K.A., Siagné, Z.H., Koffi, G.S.R. and Ouattara, Z. (2026) New U-Pb Zircon Evidence for Paleoarchean Crustal Inheritance in the Kenema-Man Domain, Western Côte d'Ivoire. *International Journal of Geosciences*, **17**, 652-670.
https://doi.org/10.4236/ijg.2026.179031

**Received:** July 29, 2026
**Accepted:** September 15, 2026
**Published:** September 18, 2026



## Abstract

The Archean evolution of the Kenema-Man Domain remains a key issue for understanding the early growth of the West African Craton (WAC), particularly in western Côte d'Ivoire where the oldest crustal components remain poorly constrained. This study presents new in situ zircon U-Pb LA-ICP-MS geochronological data from two Archean gneisses (NID-1 paragneiss and TRO-4 anatectic orthogneiss) collected in the Man region, with the aim of refining the timing of early crustal evolution and subsequent tectono-metamorphic events. Zircons from the NID-1 paragneiss define several Archean age components. Older ages between ca. 3164 ± 41 Ma and 3089 ± 23 Ma are interpreted primarily as inherited and/or detrital zircon components derived from older crustal sources. Younger ages between ca. 2895 ± 18 Ma and 2820 ± 30 Ma occur in both zircon rims and cores; they may therefore record a composite signal involving late Archean zircon growth or recrystallization as well as inherited or detrital input. In the TRO-4 anatectic orthogneiss, seven analyses previously grouped at 3320 ± 47 Ma yield a MSWD of 6.11, indicating significant excess scatter and showing that this group does not represent a single statistically homogeneous crystallization event. Nevertheless, the oldest individual analysis yields 3342 ± 18 Ma and documents the preservation of Paleoarchean zircon components in western Côte d'Ivoire. Additional zircon populations at ca. 3.20 and 3.08 Ga record younger Archean components. Zircon Th/U ratios, together with cathodoluminescence textures, indicate predominantly magmatic zircon crystallization with variable later modification. These new data strengthen the evidence for Paleoarchean crustal inheritance in the

Man region and document a prolonged history of Archean crustal growth and reworking within the Kenema-Man Domain.

**Keywords**

Kenema-Man, Paleoarchean, U-Pb Zircon, Gneiss, Crustal Evolution, WAC

## 1. Introduction

The Archean Eon represents nearly half of Earth's geological history and records the earliest stages of continental crust formation and stabilization. It is widely accepted that between 50% and 75% of the present-day continental crust was generated during the Archean through repeated episodes of mantle-derived magmatism, crustal differentiation and reworking [1]-[4]. Understanding the timing and mechanisms of Archean crustal evolution therefore remains fundamental for reconstructing the early evolution of the Earth's lithosphere.

Within the West African Craton (WAC), the Kenema-Man Domain preserves one of the largest exposures of Archean crust in Africa (**Figure 1**). This domain extends across Sierra Leone, Liberia, Guinea and western Côte d'Ivoire and consists predominantly of high-grade gneisses, granitoids and supracrustal rocks that record a prolonged history of magmatism, metamorphism and crustal reworking [5]-[7]. Early studies subdivided the Archean evolution of this region into the Leonian and Liberian events, whereas more recent investigations emphasize a more complex evolution involving multiple episodes of crustal growth and reworking rather than two discrete orogenic events [5] [7]-[10].

Significant progress has been made in constraining the Archean evolution of the Kenema-Man Domain through U-Pb zircon geochronology, Sm-Nd isotopes and whole-rock geochemistry [9] [11] [12]. These studies indicate that major crust-forming events occurred between approximately 3500 and 2800 Ma, while Sm-Nd model ages suggest the presence of even older crustal components. Nevertheless, whether inherited zircon populations record isolated remnants of ancient crust or evidence for a more widespread Paleoarchean basement beneath the Ivorian part of the Kenema-Man Domain remains unresolved.

The Man region of western Côte d'Ivoire contains extensive exposures of granulitic paragneisses, anatectic orthogneisses and associated high-grade metamorphic rocks that have long been regarded as key lithologies for investigating Archean crustal evolution [8] [11] [13]. However, most previous geochronological studies relied on conventional isotopic techniques, whereas in situ LA-ICP-MS zircon U-Pb data remain scarce for these lithologies. In this study, we present new in situ LA-ICP-MS zircon U-Pb ages obtained from a granulitic paragneiss (NID-1) and an anatectic orthogneiss (TRO-4) collected from the western Ivorian part of the Kenema-Man Domain. Petrographic observations, cathodoluminescence imaging and zircon geochronology are combined to characterize the zircon populations preserved in these rocks and to evaluate their significance for the Archean evolution of the region. Particular attention is given to identifying evidence for Paleoarchean crustal inheritance and younger Archean reworking and discussing its implications for the early crustal evolution of the southern West African Craton.

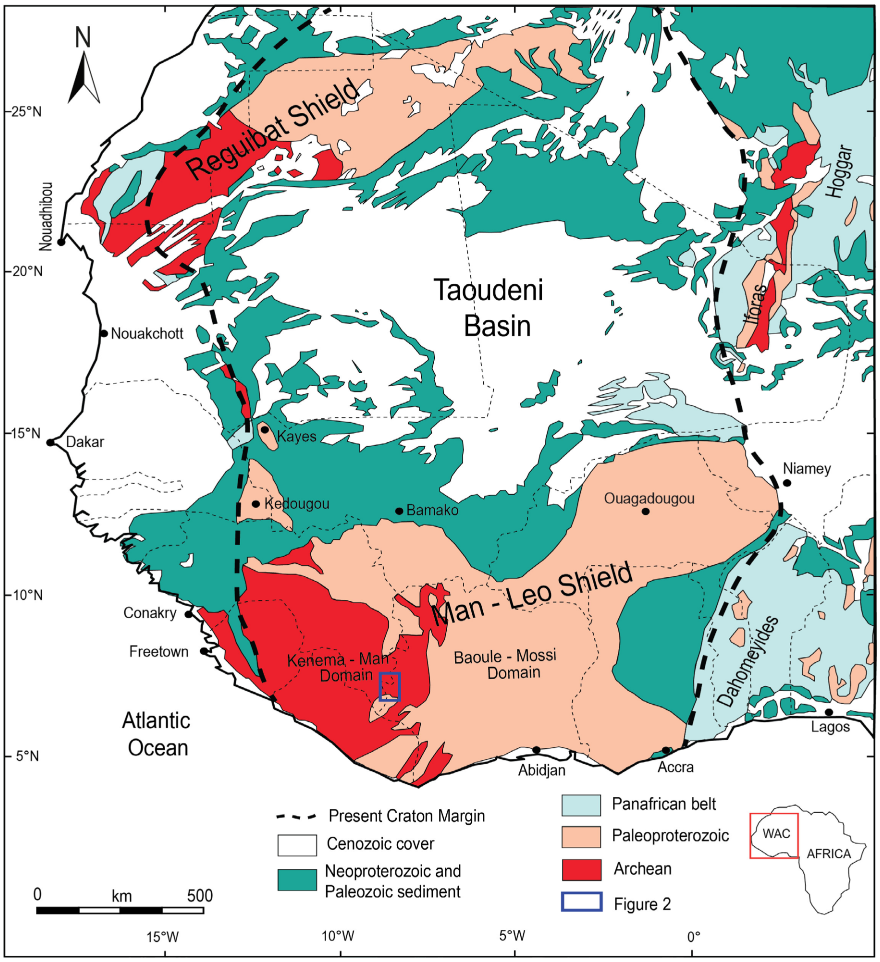


**Figure 1.** Simplified geological map of the West African Craton (WAC) showing the main Archean and Paleoproterozoic domains, surrounding sedimentary basins and Pan-African belts. The blue rectangle indicates the location of the study area in western Côte d'Ivoire. Modified after [14].

## 2. Geology of Study Area

The Archean domain in Côte d'Ivoire, also known as the Kenema-Man, occupies nearly the entire territory west of the Sassandra Fault (**Figure 2**). It has been shaped by two major geological ages: the Leonian (3400 to 3000 Ma) and the Liberian (2900 to 2700 Ma) [5] [9] [11] [15]-[18]. The Leonian period is characterized by significant magmatic accretion, while the Liberian corresponds to an orogenic phase that typically metamorphoses Leonian formations [6] [19]. But [7] [9] argue that the stratigraphic terms "Leonian" and "Liberian" are no longer relevant, as they appear redundant and do not reflect genuine orogenic events. Consequently, they favor an approach based on lithology and geochronology, which allows the distinction of four major units within the Archean domain. It should be noted, first, that a TTG suite dated between 3500 and 3600 Ma is identified in the eastern part of the domain [12] [20]. Subsequently, the TTG gneisses, which are predominant and dated between 3260 and 2850 Ma, reveal the presence of supracrustal rocks organized into linear belts that were folded and metamorphosed into amphibolite and granulite [11] [18] [21]-[23]. Moreover, a suite of Late Archean granitoids was formed through partial melting of the TTG gneisses during a craton-scale event of deformation, metamorphism, and partial melting around 2800 Ma [24]. Finally, this episode marks the definitive stabilization of the craton, thereby sealing the geological and structural evolution of the region.

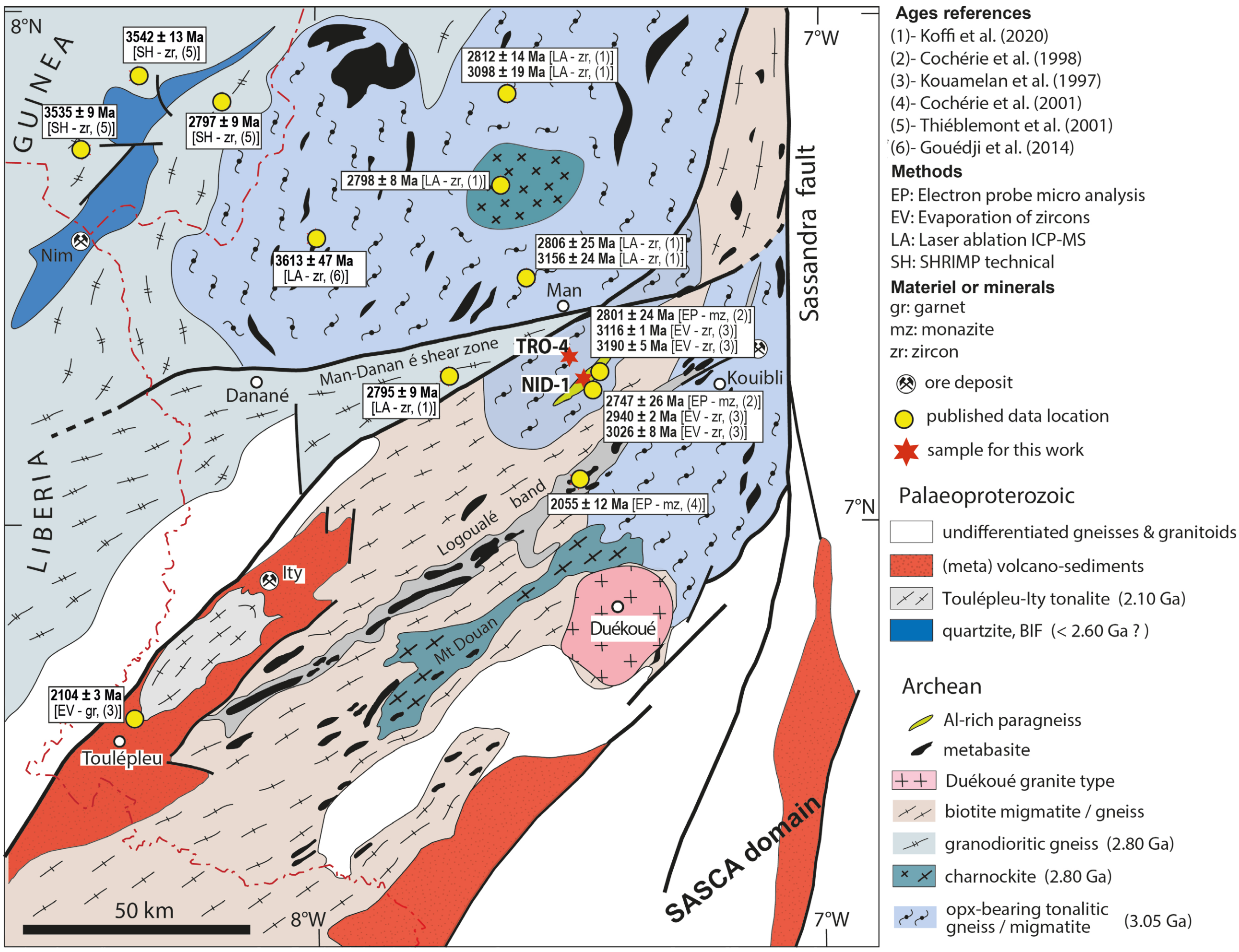


**Figure 2.** Geological map of the Kenema-Man domain in western Côte d'Ivoire showing the distribution of the main Archean and Paleoproterozoic lithological units, major tectonic structures, published geochronological data (yellow circles), and the locations of samples analyzed in this study (red stars). The map highlights the position of the NID-1 paragneiss and TRO-4 orthogneiss samples within the Archean basement. Modified after [6].

The Man domain itself extends between latitudes 6˚ and 8˚N and lithologically subdivides into two parts. To the north lies the zone of grey granulitic gneisses, separated by the Man-Danané shear zone from the anatectic complex to the south

[6] [11] [25]. Within the second zone, [8] distinguish: i) domain A, characterized by proterozoic metamorphized volcano-sediments, and ii) domain B, known as the Logoualé Band, composed of biotite-bearing migmatites [5]. To the East of the Logoualé Band, rocks are strongly deformed and exhibit a foliated appearance. Numerous basic bodies, included within the migmatitic gneisses containing hypersthene, bear witness to this deformation. To the north of the Logoualé Band, in addition to migmatite gneisses, there are units composed of anatectic mobilisate associated with metasediments. [8] refers to these as "panel of aluminous-rich paragneiss". Our sampling during this study primarily focuses on these metasediments around the locality of Man (**Figure 2**). The investigated rocks crop out in the vicinity of the villages of Trokpadrou and Nidrou, approximately 10 km and 14 km northwest of Man, respectively. The sampling sites are indicated on the geological map by samples NID-1 and TRO-4, and their geographic coordinates and lithological characteristics are summarized in **Table 1**. These gneisses, which are granulitic rocks, have been dated to approximately 2850 Ma using the electron microprobe by Th-U total lead determination method applied on monazite [11] [13]. South of the Man-Danané shear zone, the Archean rocks underwent intense metamorphism during the Paleoproterozoic, although relics of granulite facies are still preserved.

**Table 1.** Location, cartographic units, and lithological characteristics of the representative Archean gneiss samples analyzed in this study. Geographical coordinates are based on WGS 84, and elevation is expressed in meters.

| Samples | Cartographic units | Lithology | Latitude | Longitude | Elevation |
|---|---|---|---|---|---|
| NID-1 | Archean Al-rich paragneiss [8] [11] | Paragneiss | 7˚18'01.58"N | 7˚26'39.91"W | 252 |
| TRO-4 | Archean Opx-bearing tonalitic gneiss [11] [13] | Orthogneiss | 7˚19'03.98"N | 7˚28'12.00"W | 396 |

Furthermore, [26] suggested that the charnockites in the Man region have protoliths as the tonalitic gneisses of Balmer, dated at 3207 ± 7 Ma using the U-Pb method within the SASCA domain (Sassandra-Cavally). The presence of the Ity-Toulepleu Birimian unit, formed at 2100 Ma, within a syntectonic context in a weakened Archean crust [6] [27], constitutes a particular feature of this western region.

## 3. Analytical Methods

Field investigations were carried out in the Archean basement of the Man region, western Côte d'Ivoire, with the objective of identifying lithologies suitable for constraining the origin and evolution of the Archean crust. Based on these observations, two representative samples were selected for detailed petrographic and geochronological investigation (**Table 1**). NID-1 sample corresponds to paragneiss, whereas TRO-4 represents an anatectic orthogneiss. These lithologies were chosen because: i) the paragneiss is expected to preserve inherited detrital zircon populations derived from older crustal sources, ii) the orthogneiss records partial melting and reworking of pre-existing felsic crust.

Approximately 5 kg of fresh, unweathered rock was collected from each site to ensure recovery of a sufficient zircon population for geochronological analysis. Standard thin sections (30 µm) were prepared at *Institut National Polytechnique Félix Houphouët-Boigny*, Yamoussoukro (INP-HB). Petrographic observations were conducted under transmitted and cross-polarized light microscopy and particular attention was paid to mineral relationships, metamorphic textures, and evidence of partial melting, in order to establish the petrographic framework for interpreting zircon U-Pb geochronological data.

The selected samples were subsequently subjected to processing and analysis procedures for U-Th-Pb data on zircon using laser ablation (LA-ICP-MS) at the University of Rennes, France. The preparation of the selected samples began with a crushing and sieving phase to obtain a mineral fraction with a diameter inferior to 500 µm. After washing on a "Wifley table", the pulp underwent density and magnetic separation (using diiodomethane and the Frantz isodynamic separator, respectively) to collect a heavy mineral concentrate. From this second fraction, zircons (the target minerals) were carefully handpicked and isolated under a binocular loupe. Subsequently, the zircons were mounted on resin studs and delicately polished using 1 µm and 6 µm diamond abrasives. Cathodoluminescence (CL) and backscattered-electron (BSE) images were used to identify suitable domains for laser ablation. The laser analytical conditions were applied according to [5] and are summarized in **Table 2**. Analyses were performed using an ESI NWR193UC excimer laser system coupled to an Agilent 7700x quadrupole ICP-MS. The instrument was fitted with a dual pumping configuration to optimize ion transmission and improve analytical sensitivity. GJ-1 zircon (accepted age 609 ± 1 Ma) was used as the primary calibration reference material, whereas 91500, Plesovice and Temora were analysed as secondary reference materials for quality control. During the analytical session, GJ-1 yielded a weighted mean $^{206}Pb/^{238}U$ age of 601.8 ± 2.4 Ma (MSWD = 0.79; probability of fit = 0.72). Propagated uncertainties were included during data reduction. No common-Pb correction was applied during data reduction. Concordance was calculated as ($^{207}Pb/^{206}Pb$ age/$^{206}Pb/^{238}U$ age) × 100, and analyses with concordance values below 95% were excluded from age interpretation [28] [29]. Concordia diagrams and age histograms were generated using Isoplot 4.15 software, with uncertainties reported at $2\sigma$ [30].

**Table 2.** Analytical conditions and instrumental setup for LA-ICP-MS zircon U-Pb geochronology at the University of Rennes, France.

| Laser-ablation system ESI NWR193UC | |
|---|---|
| Laser type/wavelength | Excimer 193 nm |
| Pulse duration | <5 ns |
| Energy density on target | ~7 J/cm |
| $ThO^+/Th^+$ | < 0.5% |
| He gas flow | ~800 ml/min |

**Continued**

| | |
|---|---|
| $N_2$ gas flow | 4 ml/min |
| Laser repetition rate | 3 - 5 Hz (zircon) |
| Laser spot size | 26 - 44 µm (zircon) |
| ICP-MS Agilent 7700× | |
| RF power | 1350 W |
| Sampling depth | 5.0 - 5.5 mm (optimized daily) |
| Carrier gas flow (Ar) | ~0.85 l/min (optimized daily) |
| Coolant gas flow | 16 l/min |
| Data acquisition protocol | Time-resolved analysis |
| Scanning mode | Peak hopping, one point per peak |
| Detector mode | Pulse counting, dead time correction applied, and analog mode when signal intensity > ~106 cps |
| Isotopes determined | $^{204}$(Hg + Pb), $^{206}$Pb, $^{207}$Pb, $^{208}$Pb, $^{232}$Th, $^{238}$U |
| Dwell time per isotope | 10 ms (30 ms for $^{207}$Pb) |
| Sampler, skimmer cones | Ni |
| Standard samples | GJ1, Temora-2, Plesovice, 91500 |
| Extraction lenses | X type |

# 4. Results

## 4.1. Field Observations and Petrography

- Paragneiss

The NID-1 sample is a high-grade aluminous paragneiss exhibiting a well-developed gneissic foliation striking approximately N 45˚ and dipping 80˚ SE. The foliation is defined by alternating quartz-rich and biotite-rich layers and is locally affected by tight to isoclinal folds (**Figure 3(a)**, **Figure 3(b)**). In thin section, the rock displays a medium-grained granolepidoblastic texture, except for garnet porphyroblasts, and consists predominantly of quartz, garnet, biotite and sillimanite, with subordinate feldspar (**Figure 3(c)**). Quartz forms elongated ribbons parallel to the foliation, commonly arranged in bands of 1 - 2 mm thick. Garnet occurs as subhedral porphyroblasts reaching up to 3 mm in diameter and commonly contains inclusions of quartz, biotite and rutile. Biotite forms reddish-brown flakes that define the rock foliation, whereas sillimanite occurs as abundant prismatic crystals preferentially associated with the biotite-rich domains. Numerous opaque minerals are also aligned parallel to the foliation. Accessory minerals include zircon, monazite and pyrite, listed in decreasing order of abundance. Zircon occurs as small prismatic to rounded grains, whereas monazite is generally associated with the biotite-rich domains. Pyrite is present as disseminated euhedral crystals throughout the rock.

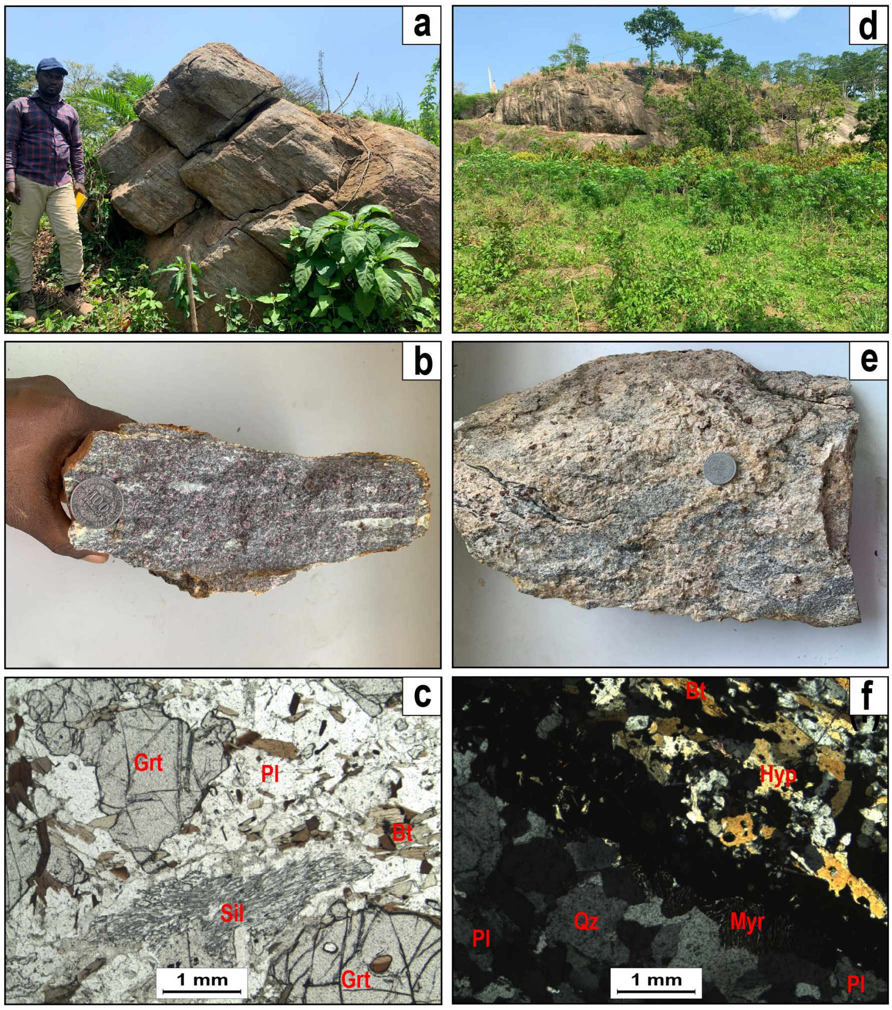


Figure 3. Field photographs and photomicrographs illustrating the petrographic features of the Archean gneiss samples analyzed in this study. (a-c) Images corresponding to NID-1 and (d-f) to TRO-4. (a) Outcrop showing subvertical gneissic foliation; (b) hand specimen with garnet porphyroblast and elongated quartz crystal; (c) photomicrograph in plane-polarized light displaying the characteristic garnet-sillimanite-biotite assemblage, indicative of a high-grade protolith; (d) dome-shaped outcrop of the TRO-4 orthogneiss; (e) hand specimen with weakly developed foliation; (f) photomicrograph in crossed-polarized light showing quartz-plagioclase-orthopyroxene-myrmekite, consistent with granulite-facies conditions.

- Orthogneiss

In the field, TRO-4 sample is spatially associated with the aluminous paragneiss described above, although the contact between the two lithologies was not observed. The rock forms strongly migmatized, dome-shaped outcrops and is composed predominantly of quartz and feldspar (>90 vol.%) (**Figure 3(d)**). Relict pockets of smoky quartz are locally preserved within the outcrop. Foliation is weakly developed owing to the scarcity of phyllosilicate minerals, whereas abundant pink K-feldspar gives the rock its characteristic grey to pink colour (**Figure 3(e)**). Under the microscope, the orthogneiss exhibits a predominantly granoblastic texture ranging from fine- to coarse-grained. Centimetre-scale leucocratic domains composed mainly of quartz and pink K-feldspar are readily distinguished from the surrounding matrix by their markedly coarser grain size (Figure 3(f)). Garnet is preferentially concentrated within these leucocratic domains, where crystals locally attain diameters of up to 1 cm. The surrounding matrix is fine-grained and contains biotite and hypersthene, imparting a pale green colour to the rock. Garnet commonly develops fine symplectitic intergrowths at contacts with quartz and biotite and locally contains fine sillimanite needles.

### 4.2. U-Pb Geochronology

- Ages of NID-1

Zircons extracted from NID-1 are approximately 200 μm long and are predominantly dark brown in transmitted light, with locally transparent central domains. Most grains display rounded terminations and contain numerous alteration zones together with small apatite inclusions. The cathodoluminescence (CL) images reveal well-developed oscillatory zoning bordered by thin luminescent rims (Figure 4). The zircon cores occupy the largest proportion of each grain and are commonly surrounded by narrow overgrowths. Sixteen *in-situ* LA-ICP-MS analyses are reported for the NID-1 paragneiss (Table 3); age interpretation follows the adopted 95% concordance criterion. The analysed zircons display Th/U ratios ranging from 0.05 to 2.28, whereas the measured $^{206}Pb/^{238}U$ ages range from 2582 to 3165 Ma. The $^{207}Pb/^{206}Pb$ ages define younger and older Archean components. The younger group is characterized by Discordia upper-intercept ages of 2895 ± 18 Ma (n = 2) and 2820 ± 30 Ma (MSWD = 0.47; n = 3). The older group yields an upper-intercept age of 3089 ± 23 Ma (MSWD = 0.88; n = 8) together with a concordant age of 3164 ± 41 Ma (MSWD = 1.7; n = 2). Spot #10, which is slightly affected by Pb loss, was excluded from further interpretation (Figure 5).

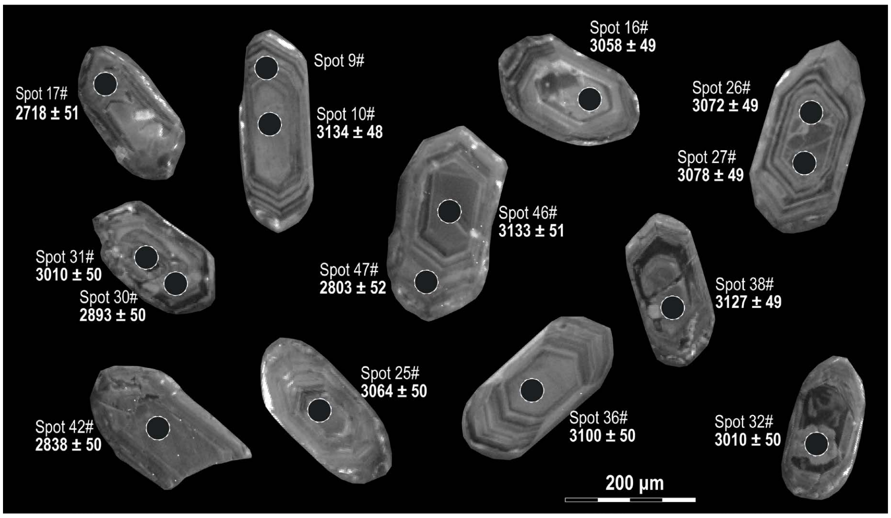


Figure 4. Cathodoluminescence (CL) images of zircon grains from the NID-1 paragneiss sample. Black circles mark the LA-ICP-MS analytical spots used for U-Pb isotope measurements. The scale bar corresponds to 200 μm.

**Table 3.** U-Pb laser ablation data on zircon from paragneiss NID-1 sample.

| Spots | Zircon | U (ppm) | Th (ppm) | Th/U | Isotopic ratios | | | | | Ages (Ma) | | | | | | Conc (%) |
|---|---|---|---|---|---|---|---|---|---|---|---|---|---|---|---|---|
| | | | | | $^{207}Pb/^{235}U$ | ±2σ (abs) | $^{206}Pb/^{238}U$ | ±2σ (abs) | Rho | $^{207}Pb/^{206}Pb$ | ±2σ | $^{207}Pb/^{235}U$ | ±2σ | $^{206}Pb/^{238}U$ | ±2σ | |
| 10# | 2.2 | 576 | 27 | 0.05 | 18.658 | 0.7 | 0.559 | 0.02 | 0.95 | 3134 | 48 | 3024 | 36 | 2862 | 86 | 95 |
| 16# | 4 | 316 | 102 | 0.32 | 19.344 | 0.73 | 0.608 | 0.02 | 0.87 | 3058 | 49 | 3059 | 37 | 3061 | 91 | 100 |
| 17# | 5.1 | 638 | 39 | 0.06 | 12.72 | 0.48 | 0.493 | 0.018 | 0.97 | 2718 | 51 | 2659 | 36 | 2582 | 79 | 95 |
| 25# | 7.2 | 497 | 900 | 1.81 | 19.162 | 0.72 | 0.6 | 0.02 | 0.89 | 3064 | 50 | 3050 | 36 | 3029 | 90 | 99 |
| 26# | 8.1 | 256 | 88 | 0.35 | 18.102 | 0.68 | 0.564 | 0.02 | 0.94 | 3072 | 49 | 2995 | 36 | 2882 | 86 | 95 |
| 27# | 8.2 | 291 | 79 | 0.27 | 19.341 | 0.73 | 0.6 | 0.02 | 0.88 | 3078 | 49 | 3059 | 36 | 3030 | 90 | 98 |
| 30# | 10 | 772 | 244 | 0.32 | 14.687 | 0.55 | 0.511 | 0.019 | 0.99 | 2893 | 50 | 2795 | 36 | 2662 | 81 | 95 |
| 31# | 11 | 223 | 75 | 0.33 | 18.183 | 0.68 | 0.589 | 0.02 | 0.91 | 3010 | 50 | 3000 | 36 | 2984 | 88 | 99 |
| 32# | 12 | 262 | 118 | 0.45 | 19.304 | 0.72 | 0.598 | 0.02 | 0.9 | 3079 | 49 | 3057 | 36 | 3023 | 89 | 98 |
| 36# | 14.1 | 192 | 437 | 2.28 | 18.432 | 0.7 | 0.564 | 0.02 | 0.93 | 3100 | 50 | 3013 | 37 | 2883 | 86 | 95 |
| 38# | 15.1 | 129 | 50 | 0.39 | 20.827 | 0.78 | 0.627 | 0.02 | 0.85 | 3127 | 49 | 3131 | 36 | 3136 | 92 | 100 |
| 42# | 17.2 | 624 | 19 | 0.03 | 14.987 | 0.56 | 0.54 | 0.02 | 0.99 | 2838 | 50 | 2814 | 36 | 2782 | 83 | 98 |
| 46# | 18.2 | 174 | 39 | 0.22 | 21.152 | 0.81 | 0.634 | 0.02 | 0.82 | 3133 | 51 | 3146 | 37 | 3165 | 93 | 100 |
| 47# | 19 | 197 | 121 | 0.62 | 13.877 | 0.53 | 0.51 | 0.019 | 0.98 | 2803 | 52 | 2741 | 36 | 2658 | 80 | 95 |
| 49# | 21 | 467 | 134 | 0.29 | 15.736 | 0.59 | 0.547 | 0.02 | 0.98 | 2895 | 51 | 2861 | 36 | 2813 | 84 | 97 |
| 51# | 24 | 580 | 73 | 0.13 | 13.646 | 0.51 | 0.497 | 0.018 | 0.97 | 2820 | 51 | 2725 | 36 | 2600 | 78 | 95 |

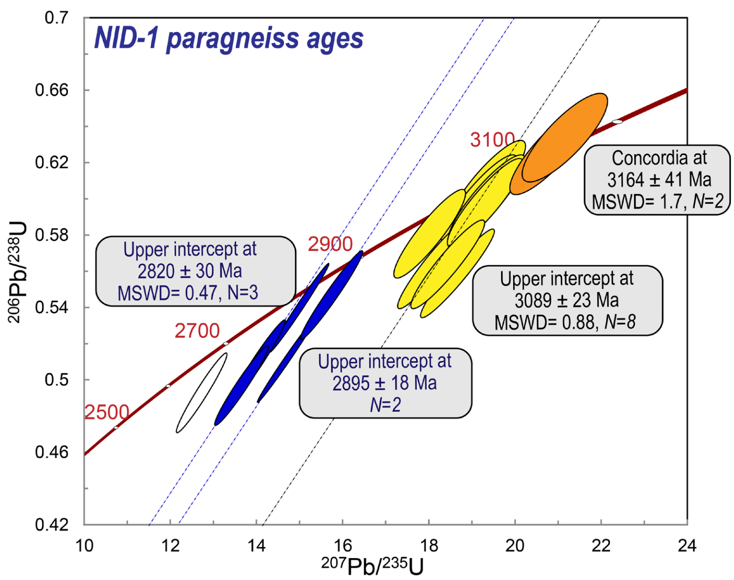


**Figure 5.** Concordia diagram for zircon U-Pb analyses from the NID-1 paragneiss sample. Ellipses represent individual spot analyses, with colors distinguishing analytical reliability and age groups (white = excluded/unreliable analyse, dark blue = younger Archean group, yellow = older Archean group, orange = oldest concordant analyses).

- Ages of TRO-4

Zircons separated from the TRO-4 anatectic orthogneiss are predominantly rounded to blunt and generally exhibit a dark appearance in transmitted light. Cathodoluminescence images systematically reveal the presence of inherited cores surrounded by overgrowths with diffuse boundaries (**Figure 6**). In most grains, the inherited cores account for more than 75% of the zircon surface area. Oscillatory zoning is locally preserved within the overgrowths and is best observed in a few relatively transparent zircon grains. Seventeen in situ LA-ICP-MS analyses performed on sixteen zircon grains are reported in **Table 4** and age interpretation follows the adopted 95% concordance criterion. The analysed zircons display Th/U ratios ranging from 0.11 to 2.02, with most $^{207}Pb/^{206}Pb$ ages older than 3000 Ma. The oldest individual analysis yielded a $^{207}Pb/^{206}Pb$ age of 3342 ± 18 Ma. The Concordia diagram shows principal Archean age components at ca. 3082 ± 20 Ma, 3204 ± 21 Ma, and 3.32 Ga. Seven analyses yield a mean age of 3320 ± 47 Ma (MSWD = 6.11). The relatively high MSWD indicates significant dispersion among these analyses, suggesting that they do not define a statistically homogeneous zircon population (**Figure 7**).

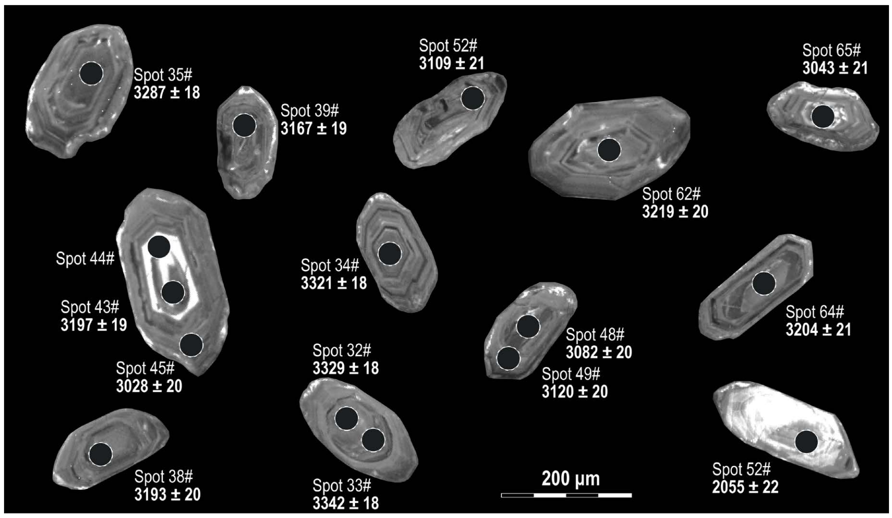


**Figure 6.** Cathodoluminescence (CL) images of zircon grains from the TRO-4 orthogneiss sample. Black circles mark the LA-ICP-MS analytical spots used for U-Pb isotope measurements. The scale bar corresponds to 200 μm.

**Table 4.** U-Pb laser ablation data on zircon from anatectic orthogneiss TRO-4.

| Spots | Zircon | U (ppm) | Th (ppm) | Th/U | Rapports isotopiques | | | | | Ages en Ma | | | | | | Conc (%) |
|---|---|---|---|---|---|---|---|---|---|---|---|---|---|---|---|---|
| | | | | | $^{207}Pb/^{235}U$ | ±2σ (abs) | $^{206}Pb/^{238}U$ | ±2σ (abs) | Rho | $^{207}Pb/^{206}Pb$ | ±2σ | $^{207}Pb/^{235}U$ | ±2σ | $^{206}Pb/^{238}U$ | ±2σ | |
| 32# | 14.1 | 68 | 55 | 0.81 | 24.949 | 0.33 | 0.661 | 0.008 | 0.95 | 3329 | 18 | 3306 | 13 | 3269 | 32 | 99 |
| 33# | 14.2 | 67 | 49 | 0.74 | 25.333 | 0.34 | 0.665 | 0.008 | 0.95 | 3342 | 18 | 3321 | 13 | 3287 | 32 | 99 |
| 34# | 15 | 61 | 45 | 0.74 | 24.797 | 0.33 | 0.660 | 0.008 | 0.94 | 3321 | 18 | 3300 | 13 | 3266 | 32 | 99 |
| 35# | 16 | 41 | 35 | 0.85 | 24.102 | 0.32 | 0.655 | 0.008 | 0.94 | 3287 | 18 | 3273 | 13 | 3249 | 32 | 100 |
| 38# | 19 | 16 | 7 | 0.46 | 22.341 | 0.31 | 0.645 | 0.008 | 0.93 | 3193 | 20 | 3199 | 13 | 3208 | 33 | 100 |
| 39# | 20 | 32 | 25 | 0.77 | 20.654 | 0.28 | 0.606 | 0.008 | 0.93 | 3167 | 19 | 3123 | 13 | 3054 | 31 | 99 |
| 43# | 23 | 212 | 369 | 1.74 | 10.402 | 0.14 | 0.300 | 0.004 | 0.93 | 3197 | 19 | 2471 | 13 | 1689 | 19 | 98 |
| 45# | 25 | 53 | 33 | 0.62 | 17.709 | 0.24 | 0.567 | 0.007 | 0.92 | 3028 | 20 | 2974 | 13 | 2895 | 30 | 98 |
| 48# | 26 | 32 | 26 | 0.8 | 19.643 | 0.28 | 0.608 | 0.008 | 0.92 | 3082 | 20 | 3074 | 14 | 3062 | 31 | 100 |
| 49# | 27 | 59 | 68 | 1.14 | 20.451 | 0.28 | 0.618 | 0.008 | 0.92 | 3120 | 20 | 3113 | 13 | 3103 | 31 | 100 |
| 52# | 30 | 629 | 655 | 1.01 | 6.142 | 0.09 | 0.351 | 0.004 | 0.91 | 2055 | 22 | 1996 | 12 | 1940 | 21 | 97 |

Continued

| | | | | | | | | | | | | | | | | |
|---|---|---|---|---|---|---|---|---|---|---|---|---|---|---|---|---|
| 61# | 33.1 | 37 | 40 | 1.08 | 19.348 | 0.28 | 0.589 | 0.008 | 0.89 | 3109 | 21 | 3059 | 14 | 2985 | 31 | 98 |
| 62# | 34 | 135 | 70 | 0.52 | 21.621 | 0.31 | 0.614 | 0.008 | 0.89 | 3219 | 20 | 3167 | 14 | 3085 | 31 | 98 |
| 64# | 35 | 120 | 62 | 0.52 | 19.915 | 0.29 | 0.571 | 0.007 | 0.88 | 3204 | 21 | 3087 | 14 | 2912 | 30 | 96 |
| 65# | 36 | 238 | 25 | 0.11 | 16.039 | 0.23 | 0.509 | 0.007 | 0.88 | 3043 | 21 | 2879 | 14 | 2651 | 28 | 95 |
| 66# | 37 | 237 | 479 | 2.02 | 19.933 | 0.29 | 0.562 | 0.007 | 0.88 | 3232 | 21 | 3088 | 14 | 2873 | 30 | 96 |
| 67# | 38 | 280 | 486 | 1.74 | 16.549 | 0.24 | 0.537 | 0.007 | 0.88 | 3006 | 21 | 2909 | 14 | 2772 | 29 | 97 |

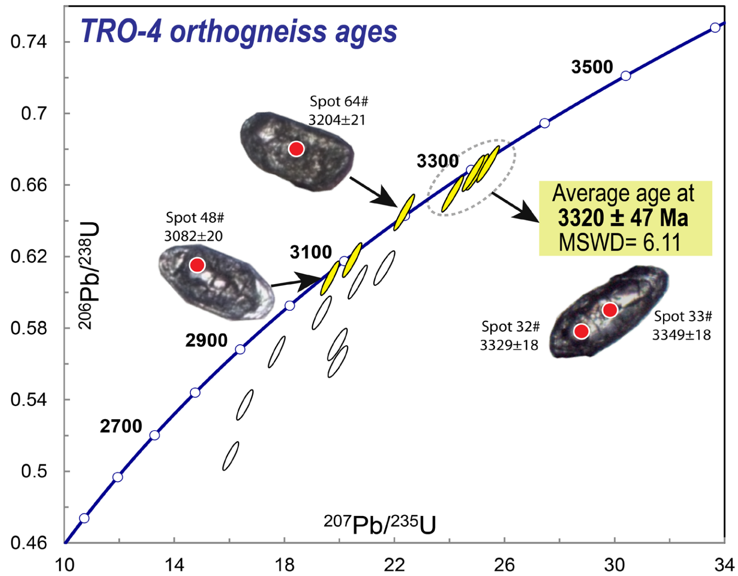


Figure 7. Concordia diagram of zircon U-Pb analyses from the TRO-4 orthogneiss. Ellipses represent individual spot analyses, with yellow indicating Archean zircon and black marking unreliable spots. Red circles show the locations of LA-ICP-MS analyses on representative grains. Zircon images are captured from transmitted light.

## 5. Discussion

### 5.1. Nature and Significance of the Zircon Populations

The zircon populations identified in the NID-1 paragneiss and TRO-4 orthogneiss record a complex Archean history involving several episodes of zircon crystallization and subsequent crustal reworking. Cathodoluminescence images reveal large cores surrounded by narrow overgrowth rims in many grains, indicating that several generations of zircon growth may be preserved within individual crystals. In the NID-1 paragneiss, the rounded to subrounded morphology of many grains and the sedimentary origin of the protolith require the U-Pb ages to be interpreted primarily as inherited and/or detrital-source ages unless independent evidence demonstrates a single magmatic crystallization event [31].

The analysed zircons display Th/U ratios ranging from 0.05 to 2.28 in the NID-1 paragneiss and from 0.11 to 1.74 in the TRO-4 orthogneiss. Most analyses yield Th/U values greater than 0.1, a range commonly associated with magmatic zircon, whereas lower values may reflect zircon growth or recrystallization under metamorphic conditions. These criteria indicate a predominantly magmatic origin for many zircon domains, although later high-grade metamorphic modification is also recorded [32]-[36] (**Figure 8**). In NID-1, ages close to 2.82 Ga occur partly on zircon rims, which is compatible with late Archean zircon growth or recrystallization, but similar ages also occur in zircon cores. The ca. 2.82 Ga component is therefore interpreted cautiously as a composite record that may include metamorphic overgrowth/recrystallization together with inherited or detrital zircon components.

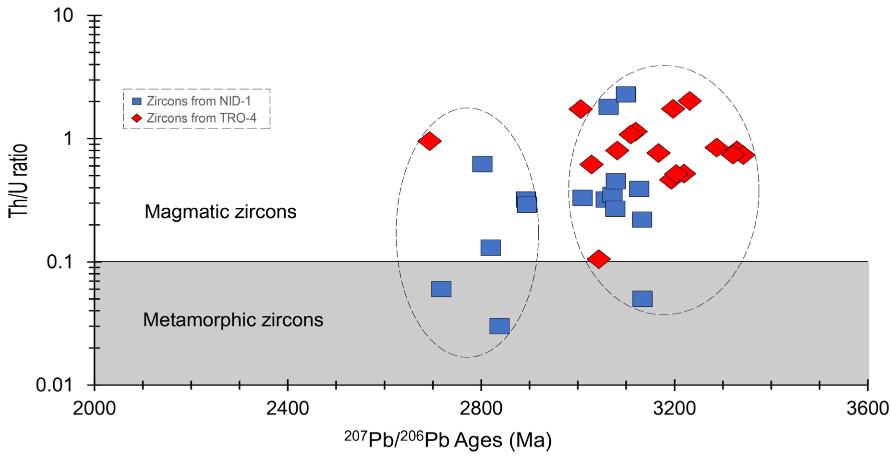


**Figure 8.** Plot of Th/U ratios versus $^{207}Pb/^{206}Pb$ ages for zircon grains from the NID-1 paragneiss (blue squares) and the TRO-4 orthogneiss (red diamonds). Magmatic and metamorphic zircon origins are distinguished by a Th/U ratio threshold of 0.1. Two age clusters are highlighted by dashed ellipses: ~2700 - 2900 Ma and ~3100 - 3320 Ma, reflecting distinct zircon growth episodes recorded in the studied samples.

The coexistence of several Archean age components within the studied zircon populations indicates incorporation and reworking of crustal material of different ages. In the paragneiss, these ages primarily constrain the ages of zircon source components rather than a unique crystallization age of the sedimentary protolith. In the orthogneiss, the age spectrum likewise records inheritance and subsequent crustal reworking. These relationships are discussed below in the context of the Archean development of the Kenema-Man Domain.

## 5.2. Evidence for Paleoarchean Crustal Inheritance in Western Côte d'Ivoire

The zircon U-Pb data provide new constraints on the Archean evolution of the Kenema-Man Domain in western Côte d'Ivoire. The oldest individual analysis from TRO-4 yields a Paleoarchean $^{207}Pb/^{206}Pb$ age of 3342 ± 18 Ma. The seven analyses yielding a mean age of 3320 ± 47 Ma are characterized by a relatively high MSWD of 6.11, indicating that they do not constitute a statistically homogeneous zircon population. Rather than representing a single discrete crystallization event, this dispersion may record zircon crystallization during a protracted period of Paleoarchean crustal accretion and growth. The ca. 3.32 Ga age is therefore considered to represent an ancient crustal component preserved within the TRO-4 orthogneiss, rather than a precisely defined single magmatic event. This interpretation is consistent with previous isotopic evidence suggesting the presence of ancient crust beneath the Man Domain. Whole-rock Sm-Nd model ages between 3300 and 3200 Ma reported for granulitic grey gneisses and related lithologies have long suggested the existence of older crustal components, although direct zircon evidence has remained limited. [11] interpreted these Nd model ages as recording an early stage of continental crustal growth in the Man Rise. Additional support comes from the Balmer tonalitic gneiss, for which [26] obtained an *in-situ* LA-ICP-MS zircon age of 3207 ± 7 Ma, interpreted as the crystallization age of its magmatic protolith. That study proposed that the Balmer gneiss represents one of the oldest juvenile crustal units currently recognized in Côte d'Ivoire and suggested that even older rocks might still be discovered within the Man Domain. The Paleoarchean zircon components documented here extend the recognized record of ancient crustal material in western Côte d'Ivoire.

At the scale of the southern West African Craton, these new data are consistent with the regional chronological framework summarized by [7], who recognized crust-forming episodes between approximately 3200 and 3000 Ma, together with evidence for older Paleoarchean rocks locally preserved in Guinea and neighbouring regions. Although ages approaching 3.5 Ga have not been identified in the present dataset, unlike the older continental crust reported from Guinea [12] [18], the zircon populations described in this study confirm that the Archean basement of western Côte d'Ivoire preserves a long history of crustal evolution, marked both by the retention and subsequent reworking of ancient continental material.

### 5.3. Implications for the Archean Evolution of the Kenema-Man Domain

The zircon age spectra obtained from the paragneiss and anatectic orthogneiss indicate that the Archean basement of western Côte d'Ivoire preserves a record of multiple crustal events spanning more than 500 Ma. Rather than reflecting a single episode of crust formation, the occurrence of Paleoarchean zircon components together with younger ca. 3.32, 3.20, 3.08 and 2.82 Ga ages suggests a long-lived history involving magmatic activity, inheritance, crustal reworking and high-grade metamorphism.

The oldest zircon group identified in this study indicates that Paleoarchean crustal material was already present in the western part of the Man region Domain by at least ca. 3.34 Ga. Younger zircon age components document additional episodes affecting this crust during the Meso- to Neoarchean [5] [19] [37]. The ca. 2.82 Ga ages recorded in NID-1 occur in both rims and cores and therefore cannot be attributed unequivocally to a single metamorphic event; they may represent a composite record of late Archean zircon growth or recrystallization and inherited/detrital input. Although the precise tectonic significance of each age component cannot be established from U-Pb geochronology alone, the overall age distribution is consistent with repeated growth and reworking of pre-existing continental material. These results agree with regional models proposed for the Kenema-Man Domain, in which Archean crust developed through successive magmatic and metamorphic events prior to the Paleoproterozoic assembly of the West African Craton. Similar age ranges have been reported from neighbouring regions of Liberia, Sierra Leone and Guinea, indicating that the Archean terranes of the southern West African Craton shared a broadly comparable geological evolution. The occurrence of Paleoarchean zircon inheritance in western Côte d'Ivoire therefore strengthens the regional continuity of this ancient crustal domain.

Although the present study is based on two representative samples, it provides new geochronological evidence that complements previous isotopic and geochronological investigations in western Côte d'Ivoire. Additional U-Pb analyses combined with Lu-Hf isotopic data from zircon and broader sampling across the Man Domain will be essential to distinguish juvenile crustal growth from crustal reworking and to refine the spatial distribution and evolution of the Paleoarchean basement.

## 6. Conclusions

This study presents new in situ LA-ICP-MS zircon U-Pb ages obtained from a granulitic paragneiss (NID-1) and an anatectic orthogneiss (TRO-4) of the Archean Kenema-Man Domain in western Côte d'Ivoire. Combined petrographic observations, cathodoluminescence imaging and zircon geochronology reveal several Archean zircon age components and document a prolonged history of crustal inheritance and reworking. In TRO-4, the oldest individual analysis yields 3342 ± 18 Ma, demonstrating the preservation of Paleoarchean zircon material. This result complements previous Sm-Nd model ages and zircon U-Pb data reported from the Man Domain and extends the geochronological record of ancient crustal components in this part of the southern West African Craton.

The coexistence of Paleoarchean zircon components and younger Archean age populations at approximately 3.32, 3.20, 3.08 and 2.82 Ga indicates a complex history involving inheritance, magmatism, crustal reworking and high-grade metamorphism. In the NID-1 paragneiss, the ca. 2.82 Ga component occurs in both zircon rims and cores and is therefore not interpreted as unequivocal evidence of a single metamorphic event. U-Pb zircon geochronology alone cannot fully resolve the tectonic significance of each age component, but the data reinforce evidence for the preservation and repeated reworking of ancient continental crust in western Côte d'Ivoire. Future integration of zircon Lu-Hf isotopes with expanded U-Pb sampling across the Man Domain will help distinguish juvenile crustal growth from crustal reworking and further refine the early evolution of the southern West African Craton.

## Acknowledgements

The authors gratefully acknowledge team of Laboratory of Geochronology and Geochemistry of Geosciences Rennes, France, for providing facilities for performing the zircon U-Pb LA-ICP-MS analyses and cathodoluminescence imaging. We also acknowledge all colleagues and technicians who contributed to the field campaigns, sample preparation and analytical work. Their assistance was essential to the completion of this study. Finally, we thank the anonymous reviewers whose constructive comments will contribute to improving the quality of this manuscript.

## Author Contributions

Conceptualization: W. Digbeu; methodology: A. N. Kouamelan; software: W. Digbeu; validation: K. A. N'Dri, G. S. R. Koffi, and Z. Ouattara; analysis: G. Koffi and Z. H. Siagné, Field investigation: W. Digbeu, A. N. Kouamelan, Z. H. Siagné; supervision: Z. Ouattara and A. N. Kouamelan. All authors have read and agreed to the published version of the manuscript.

## Conflicts of Interest

The authors declare that they have no known competing financial interests or personal relationships that could have appeared to influence the work reported in this paper.

## References

[1] Frost, C., Mueller, P., Mogk, D., Frost, B. and Henry, D. (2023) Creating Continents: Archean Cratons Tell the Story. *GSA Today*, **33**, 4-10. https://doi.org/10.1130/gsatg541a.1

[2] Nelson, B.K. and Depaolo, D.J. (1985) Rapid Production of Continental Crust 1.7 to 1.9 B.Y. Ago: Nd Isotopic Evidence from the Basement of the North American Mid-continent. *Geological Society of America Bulletin*, **96**, 746-754. https://doi.org/10.1130/0016-7606(1985)96<746:rpocct>2.0.co;2

[3] Rudnick, R.L. (1995) Making Continental Crust. *Nature*, **378**, 571-578. https://doi.org/10.1038/378571a0

[4] Taylor, S.R. and McLennan, S.M. (1985) The Continental Crust: Its Composition and Evolution. https://www.osti.gov/biblio/6582885

[5] Koffi, G.R., Kouamelan, A.N., Allialy, M.E., Coulibaly, Y. and Peucat, J. (2020) Re-evaluation of Leonian and Liberian Events in the Geodynamical Evolution of the Man-Leo Shield (West African Craton). *Precambrian Research*, **338**, Article 105582. https://doi.org/10.1016/j.precamres.2019.105582

[6] Pitra, P., Kouamelan, A.N., Ballèvre, M. and Peucat, J. (2010) Palaeoproterozoic High-pressure Granulite Overprint of the Archean Continental Crust: Evidence for Homogeneous Crustal Thickening (Man Rise, Ivory Coast). *Journal of Metamorphic Geology*, **28**, 41-58. https://doi.org/10.1111/j.1525-1314.2009.00852.x

[7] Rollinson, H. (2016) Archaean Crustal Evolution in West Africa: A New Synthesis of the Archaean Geology in Sierra Leone, Liberia, Guinea and Ivory Coast. *Precambrian Research*, **281**, 1-12. https://doi.org/10.1016/j.precamres.2016.05.005

[8] Camil, J., Tempier, P. and Pin, P. (1983) Age libérien des quartzites à magnétite de la région de man (Côte d'ivoire) et leur place dans l'orogène libérien, age libérien des quartzites à magnétite de la région de man (Côte d'Ivoire) et Leur Place Dans l'orogène Libérien.

[9] Rollinson, H. (2018) The Geochemical Evolution of Archaean Felsic Gneisses in the West African Craton in Sierra Leone. *Journal of African Earth Sciences*, **143**, 28-39. https://doi.org/10.1016/j.jafrearsci.2018.03.018

[10] Tempier, P. and Camil, J. (1990) Les formations archéennes au sud de la faille danamé-man, ceinture de roches vertes avortée? Publication Occasionnelle-Centre International Pour La Formation et Les Échanges Géologiques.

[11] Kouamelan, A.N., Delor, C. and Peucat, J. (1997) Geochronological Evidence for Reworking of Archean Terrains during the Early Proterozoic (2.1 Ga) in the Western Côte d'ivoire (Man Rise-West African Craton). *Precambrian Research*, **86**, 177-199. https://doi.org/10.1016/s0301-9268(97)00043-0

[12] Thiéblemont, D., Delor, C., Cocherie, A., Lafon, J.M., Goujou, J.C., Baldé, A., Bah, M., Sané, H. and Mark Fanning, C. (2001) A 3.5 Ga Granite-Gneiss Basement in Guinea: Further Evidence for Early Archean Accretion within the West African Craton. *Precambrian Research*, **108**, 179-194. https://doi.org/10.1016/s0301-9268(00)00160-1

[13] Cocherie, A., Legendre, O., Peucat, J.J. and Kouamelan, A.N. (1998) Geochronology of Polygenetic Monazites Constrained by in Situ Electron Microprobe Th-U-Total Lead Determination: Implications for Lead Behaviour in Monazite. *Geochimica et Cosmochimica Acta*, **62**, 2475-2497. https://doi.org/10.1016/s0016-7037(98)00171-9

[14] Bessoles, B. (1977) Géologie de l'Afrique. Le craton ouest-Africain, Mémoire BRGM, 1-88.

[15] Angoran, Y. and Kadio, E. (1983) Aperçu de precambrien de Côte d'Ivoire: Geologie-metallogenie. *Journal of African Earth Sciences* (1983), **1**, 167-176. https://doi.org/10.1016/0899-5362(83)90009-x

[16] Djagre, L., Koffi, B.G., Camara, M., Ouattara, G. and Agbossoumonde, Y. (2023) The Metasedimentary-Hosted Nyangoubé Gold Prospect, Northwest Côte d'ivoire: Geochemical and Mineralogical Characterization of Associated Hydrothermal Alteration. *Heliyon*, **9**, e20227. https://doi.org/10.1016/j.heliyon.2023.e20227

[17] Kouamelan, A.N., Kra, K.S.A., Djro, S.C., Paquette, J. and Peucat, J. (2018) The Logoualé Band: A Large Archean Crustal Block in the Kenema-Man Domain (Man-Leo Rise, West African Craton) Remobilized during Eburnean Orogeny (2.05 Ga). *Journal of African Earth Sciences*, **148**, 6-13. https://doi.org/10.1016/j.jafrearsci.2017.09.004

[18] Thiéblemont, D., Goujou, J.C., Egal, E., Cocherie, A., Delor, C., Lafon, J.M., *et al.* (2004) Archean Evolution of the Leo Rise and Its Eburnean Reworking. *Journal of African Earth Sciences*, **39**, 97-104. https://doi.org/10.1016/j.jafrearsci.2004.07.059

[19] Koffi, A.Y., Thébaud, N., Kouamelan, A.N., Baratoux, L., Bruguier, O., Vanderhaeghe, O., *et al.* (2022) Archean to Paleoproterozoic Crustal Evolution in the Sassandra-Cavally Domain (Côte d'ivoire, West Africa): Insights from Hf and U-Pb Zircon Analyses. *Precambrian Research*, **382**, Article 106875. https://doi.org/10.1016/j.precamres.2022.106875

[20] Barth, M.G., Rudnick, R.L., Carlson, R.W., Horn, I. and McDonough, W.F. (2002) Re Os and U Pb Geochronological Constraints on the Eclogite-Tonalite Connection in the Archean Man Shield, West Africa. *Precambrian Research*, **118**, 267-283. https://doi.org/10.1016/s0301-9268(02)00111-0

[21] De Waele, B., Lacorde, M., Vergara, F. and Chan, G. (2015) New Insights on Proterozoic Tectonics and Sedimentation along the Peri-Gondwanan West African Margin Based on Zircon U-Pb SHRIMP Geochronology. *Precambrian Research*, **259**, 156-175. https://doi.org/10.1016/j.precamres.2014.08.008

[22] Rollinson, H.R. (1978) Zonation of Supracrustal Relics in the Archaean of Sierra Leone, Liberia, Guinea and Ivory Coast. *Nature*, **272**, 440-442. https://doi.org/10.1038/272440a0

[23] Rollinson, H.R. and Cliff, R.A. (1982) New Rb-Sr Age Determinations on the Archaean Basement of Eastern Sierra Leone. *Precambrian Research*, **17**, 63-72. https://doi.org/10.1016/0301-9268(82)90154-1

[24] Billa, M., Feybesse, J., Bronner, G., Lerouge, C., Milési, J., Traoré, S., *et al*. (1999) Les formations à quartzites rubanés ferrugineux des monts nimba et du simandou: des unités empilées tectoniquement, sur un «soubassementplutonique Archéen (Craton de Kénéma-Man), lors de l'orogène éburnéen. *Comptes Rendus de l'Académie des Sciences-Series IIA-Earth and Planetary Science*, **329**, 287-294. https://doi.org/10.1016/s1251-8050(99)80248-1

[25] Gouedji, G.E.F., Ouattara, Z., N'cho, C.O., Diaby, A.J., Picard, C., Audet, M., *et al*. (2022) Archean Tonalite-Trondhjemite-Granodiorite Suites Bearing Orthopyroxene Mineral of the Bounta Region and Their Sulfide and Oxide Iron Mineralization (Western Ivory Coast). *Journal of Minerals and Materials Characterization and Engineering*, **10**, 489-504. https://doi.org/10.4236/jmmce.2022.106035

[26] Kouamelan, A.N., Djro, S.C., Allialy, M.E., Paquette, J. and Peucat, J. (2015) The Oldest Rock of Ivory Coast. *Journal of African Earth Sciences*, **103**, 65-70. https://doi.org/10.1016/j.jafrearsci.2014.12.004

[27] Egal, E., Thiéblemont, D., Lahondère, D., Guerrot, C., Costea, C.A., Iliescu, D., *et al*. (2002) Late Eburnean Granitization and Tectonics along the Western and Northwestern Margin of the Archean Kénéma-Man Domain (Guinea, West African Craton). *Precambrian Research*, **117**, 57-84. https://doi.org/10.1016/s0301-9268(02)00060-8

[28] Block, S., Ganne, J., Baratoux, L., Zeh, A., Parra-Avila, L.A., Jessell, M., *et al*. (2015) Petrological and Geochronological Constraints on Lower Crust Exhumation during Paleoproterozoic (Eburnean) Orogeny, NW Ghana, West African Craton. *Journal of Metamorphic Geology*, **33**, 463-494. https://doi.org/10.1111/jmg.12129

[29] Paton, C., Woodhead, J.D., Hellstrom, J.C., Hergt, J.M., Greig, A. and Maas, R. (2010) Improved Laser Ablation U-Pb Zircon Geochronology through Robust Downhole Fractionation Correction. *Geochemistry, Geophysics, Geosystems*, **11**, Q0AA06.

[30] Ludwig, R.K. (2003) User's Manual for Isoplot 3.00, a Geochronlogical Toolkit for Microsoft Excel, Berkeley Geochronl. *Centre Special Publication*, **4**, 25-32. https://cir.nii.ac.jp/crid/1571417126199746176

[31] Wane, O., Liégeois, J., Thébaud, N., Miller, J., Metelka, V. and Jessell, M. (2018) The Onset of the Eburnean Collision with the Kenema-Man Craton Evidenced by Plutonic and Volcanosedimentary Rock Record of the Masssigui Region, Southern Mali. *Precambrian Research*, **305**, 444-478. https://doi.org/10.1016/j.precamres.2017.11.008

[32] Kirkland, C.L., Smithies, R.H., Taylor, R.J.M., Evans, N. and McDonald, B. (2015) Zircon Th/U Ratios in Magmatic Environs. *Lithos*, **212**, 397-414. https://doi.org/10.1016/j.lithos.2014.11.021

[33] Rubatto, D. (2017) Zircon: The Metamorphic Mineral. *Reviews in Mineralogy and Geochemistry*, **83**, 261-295. https://doi.org/10.2138/rmg.2017.83.9

[34] Vavra, G., Schmid, R. and Gebauer, D. (1999) Internal Morphology, Habit and U-Th-Pb Microanalysis of Amphibolite-to-Granulite Facies Zircons: Geochronology of the Ivrea Zone (Southern Alps). *Contributions to Mineralogy and Petrology*, **134**, 380-404. https://doi.org/10.1007/s004100050492

[35] Yakymchuk, C., Kirkland, C.L. and Clark, C. (2018) Th/U Ratios in Metamorphic

Zircon. *Journal of Metamorphic Geology*, **36**, 715-737. https://onlinelibrary.wiley.com/doi/full/10.1111/jmg.12307?casa_token=_8F5g4VnN-MwAAAAA%3Ai1zFWwl0hk8zMZuEo0OOWROsQ6PLNxbeklaZV-DONrVyppOj6V42fcuEy8BGSsGTc6p9TwDPgG4lmGZyz

[36] Zieger, J., Bittner, L., Gärtner, A., Hofmann, M., Gerdes, A., Marko, L., *et al*. (2019) U-Pb Ages of Magmatic and Detrital Zircon of the Döhlen Basin: Geological History of a Permian Strike-Slip Basin in the Elbe Zone (Germany). *International Journal of Earth Sciences*, **108**, 887-910. https://doi.org/10.1007/s00531-019-01683-0

[37] Eglinger, A., Thébaud, N., Zeh, A., Davis, J., Miller, J., Parra-Avila, L.A., *et al*. (2017) New Insights into the Crustal Growth of the Paleoproterozoic Margin of the Archean Kéména-Man Domain, West African Craton (Guinea): Implications for Gold Mineral System. *Precambrian Research*, **292**, 258-289. https://doi.org/10.1016/j.precamres.2016.11.012